

Evolution of carbides and carbon content in matrix of an ultra-high carbon sintered steel during heat treatment process

Yuan-zhi Zhu^{1,2)}, Zhe Zhu²⁾, Zhi-min Yin³⁾, and Zhi-dong Xiang²⁾

1) Key Laboratory of the Ministry of Education of China for Ferrous Metallurgy and Resources Utilization, Wuhan University of Science and Technology, Wuhan 430081, China

2) School of Materials and Metallurgy, Wuhan University of Science and Technology, Wuhan 430081, China

3) School of Material Science & Engineering, Central South University, Changsha 410083, China

(Received 2008-05-18)

Abstract: DTA, thermal expansion, XRD, and SEM were used to evaluate the effect of quenching temperature on the mechanical properties and microstructure of a novel sintered steel Fe-6Co-1Ni-5Cr-5Mo-1C. Lattice parameters and the mass fraction of carbon dissolved in the matrix of the steel quenched were investigated. It is discovered that the hardness of the steel increases with quenching temperature in the range of 840-900°C and remains constant in the range of 900 to 1100°C. It decreases rapidly when the temperature is higher than 1100°C. The mass fraction of carbon dissolved in the matrix of the steel quenched at 840°C is 0.38, but when the quenching temperature is increased to 1150°C, it increases to 0.98. The carbides formed during sintering are still present at grain boundaries and in the matrix of the steel quenched at low quenching temperatures, such as 840°C. When the quenching temperature is increased to 1150°C, most of the carbides at grain boundaries are dissolved with just a small amount of spherical $M_{23}C_6$ existing in the matrix of the quenched steel.

Key words: ultra-high carbon sintered steel; heat treatment; mechanical properties; microstructure

1. Introduction

Compared with traditional cast valve seats, a PM valve seat can be mass-manufactured with a less machining and a higher material utilization ratio. Novel sintered steel for making valve seats has been developed [1-9]. In sintered steel design for making valve seats, two aspects need to be considered. The first is the need to strengthen the matrix of the steel, which probably could be achieved through the solid solution mechanism by adding a certain amount of solid solution steel elements. The second is the requirement to enhance the wear resistance by controlling the shape, size and distribution of the secondary hard phases in the matrix. The hard secondary phases can be added to the steel or directly form in-situ in the matrix of the steel during sintering. Fe-6Co-1Ni-5Cr-5Mo-1C is such a novel sintered steel developed by the authors. In the steel, nickel and a certain amount of carbon are dissolved in the matrix for solid solution strengthening. Chromium and molybdenum are added to the steel for forming carbides during sintering. Usually, the properties of the sintered steel can not meet the require-

ments of valve seat applications. Further heat treatment is necessary to improve the mechanical properties of the sintered steel. For sintered steels, quenching is a very important heat treatment procedure for increasing their hardness and the wear resistance. Among all the processing parameters, quenching temperature has great influence on the properties and microstructure of the sintered steel.

There have been some reports on the effects of quenching temperature on the properties and microstructure of ultra-high carbon steel [10-12]. However, few quantitative studies are available on the evolution of carbides and the carbon fraction in the matrix of ultra-high carbon PM steel during heat treatment process. This article presents the results of a quantitative investigation on the evolution of carbides and the change of carbon fraction at different quenching temperatures.

2. Experiment procedure

The sintered Fe-6Co-1Ni-5Cr-5Mo-1C steel was cut into specimens with a size of 10 mm×10 mm×2

mm. DTA and thermal-expansion curves were measured. In the DTA experiment, the steel was heated from room temperature to 1300°C at 20°C/min. In thermo-expansion experiment, the heating rate was 10°C/min. The quenching temperature range was determined from the results of these two experiments. The hardness was measured on the quenched steel using a Rockwell hardness tester. Specimens quenched at different temperatures were tempered. Because the maximum temperature of valve seat steel in an operating engine is slightly above 600°C, 650°C was chosen as the tempering temperature of the quenched steel. The toughness of the tempered steel was measured by Charpy impact test. Optical microscopy investigation was made on specimens etched with a solution of 3% pure nitric acid in ethanol as an etching agent. TEM observations were made on an H-800 system (Hatachi). The XRD spectrum was measured using a

D/MAX2500 system with Cu K_{α} radiation; the accelerate voltage, electric current and scanning speed used were 30 kV, 28 mA and 0.1°/min, respectively.

3. Results and discussions

3.1. DTA and thermo-expansion measurement

The DTA and thermo-expansion traces are presented in Fig. 1. It shows that the austenite start point of the steel is 770°C and the austenite end point is 820°C. More importantly, it reveals that a phase transformation occurs at 1180°C, which defines the maximum allowable heat treatment temperature for the sintered steel. The sintered steels were all quenched from temperatures lower than 1180°C. Specifically, the specimens were held for 30 min at 840, 870, 900, 950, 1000, 1050, 1100, and 1150°C, and then quenched in engine oil to room temperature.

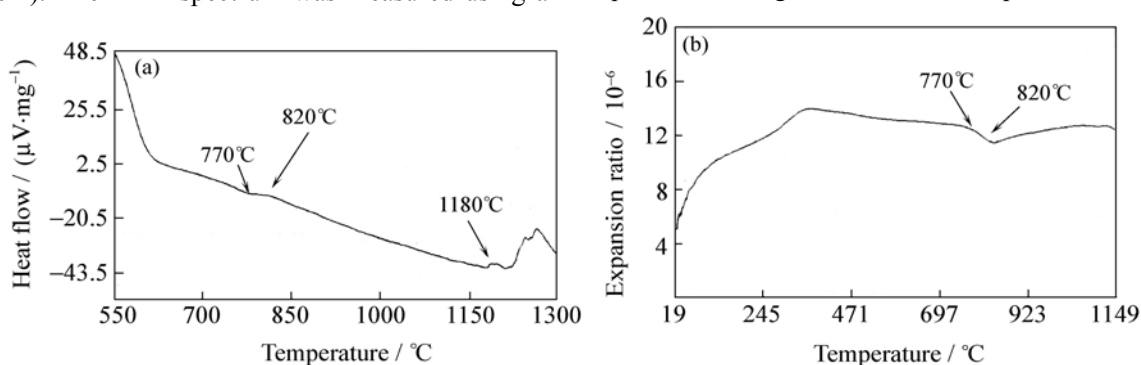


Fig. 1. Curve of DTA (a) and thermo-expansion (b).

3.2. Hardness and impact toughness of the steel

The hardness of the quenched steel is illustrated in Fig. 2. It reveals three temperature regions in which

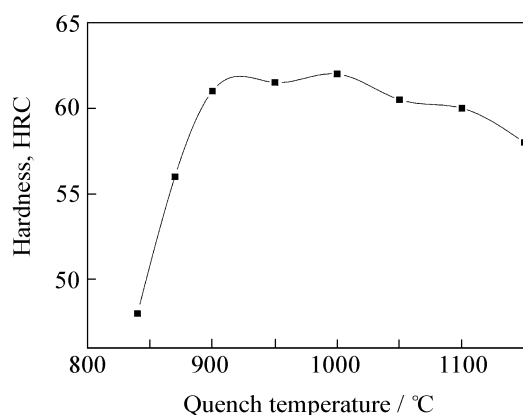


Fig. 2. Effects of quenching temperature on hardness of the Fe-6Co-1Ni-5Cr-5Mo-1C steel.

the hardness of the quenched steel shows different response to the quenching temperature. When the quenching temperature is lower than 900°C, the hardness increases with quenching temperature. At temperatures ranging from 950 to 1100°C, the hardness varies slightly with quenching temperature. But when

the quenching temperature is increased from 1100 to 1150°C, the hardness decreases to a value lower than HRC 60.

The impact toughness was measured for the steels quenched at different temperatures and then tempered at 650°C for 2 h. The results are given in Table 1.

Table 1. Effect of quenching temperature on the transverse toughness of the steel

Quenching temperature / $^{\circ}\text{C}$	Impact toughness / ($\text{J}\cdot\text{cm}^{-2}$)
900	2.77
1100	2.96
1150	2.55

3.3. Optical microscopy analysis

The optical micrographs of the quenched steel are shown in Fig. 3. It shows that carbides distribute both in the matrix and at grain boundaries and decrease as the quenching temperature increases, indicating that more carbides are dissolved into the matrix at higher temperatures. The retained austenite increases correspondingly with increasing quenching temperature, as a result of the fact that the amount of steel elements dissolved in the matrix of the steel increases with in-

creasing quenching temperature, which hinders the martensite transformation process during quenching. In the steels quenched at temperatures ranging from 840 to 1100°C, the grain size remains almost the same as the quenching temperature increases because of the

presence of stable carbides at grain boundaries, which stops the migration of grain boundaries. When the quenching temperature increases from 1100 to 1150°C, carbides are dissolved rapidly, leading to an increase in grain size.

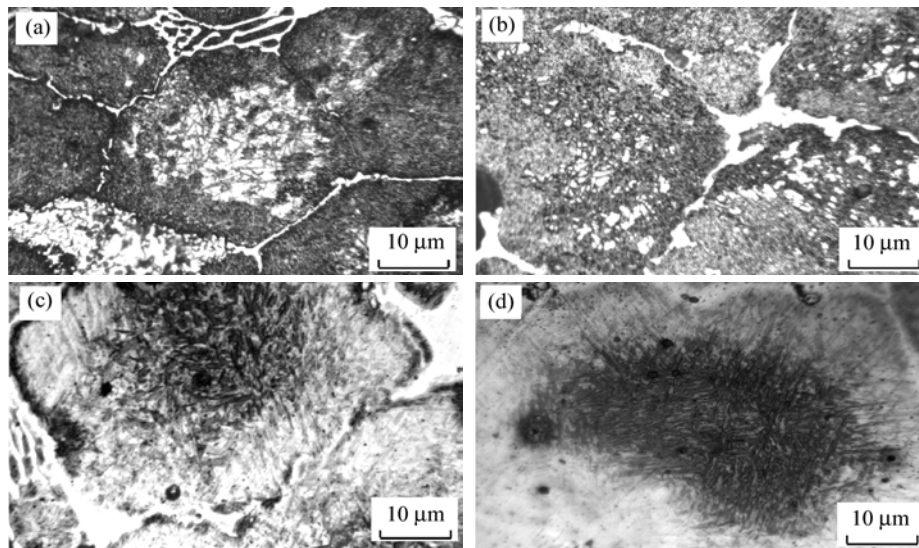


Fig. 3. Microstructures of the steel quenched at different temperatures: (a) 840°C; (b) 900°C; (c) 1100°C; (d) 1150°C.

3.4. Phase detection and precise measurement of lattice constant by XRD

XRD results (see Fig. 4) indicate that the phase in the quenched steels are mainly martensite, retained austenite, minor $(\text{Fe,Cr})_7\text{C}_3$ and Fe_2MoC . The intensity of the diffraction peaks of carbides and austenite changes with quenching temperature. The relative intensity data of austenite, $(\text{Fe,Cr})_7\text{C}_3$ and Fe_2MoC are given in Table 2. It shows that the peak intensity of the retained austenite increased with increasing quenching temperature, suggesting that the amount of the retained austenite increases. The diffraction peak intensity of Fe_2MoC decreases rapidly when the quenching temperature increases to 1100°C, indicating that the carbide Fe_2MoC dissolves quickly into the steel matrix at this temperature. However, rapid dissolution of $(\text{Fe,Cr})_7\text{C}_3$ takes place only when the quenching temperature rises to 1150°C. Therefore, the

quick dissolution of $(\text{Fe,Cr})_7\text{C}_3$ and Fe_2MoC at grain boundaries is the main cause to the increase in grain size at temperatures above 1100°C. This observation is consistent with the results of optical analysis presented in the previous section.

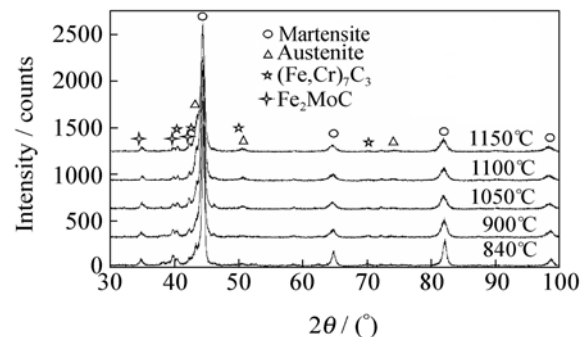


Fig. 4. XRD results of the steel quenched at different temperatures.

Table 2. Relative intensity of the strongest peaks of major phases in the steel %

Phases	Relative intensity				
	840°C	900°C	1050°C	1100°C	1150°C
Retained austenite	9.5	10.0	11.0	17.0	22.0
$(\text{Fe,Cr})_7\text{C}_3$	4.6	4.5	4.3	4.3	3.5
Fe_2MoC	5.3	4.9	4.6	3.8	2.4

The dissolution of carbides in the steel may change the lattice constant of the steel matrix. It was suggested that precise measurement of the lattice constants of the steel matrix would be helpful to understand the change of the steel's mechanical properties

with quenching temperature [13-14]. Thus, in this study, three diffraction peaks of the quenched steel at high angles were used to calculate the lattice constant using the least square method. The results for steels quenched at different temperatures are given in Table

3. It shows that the lattice constant increases with increasing quenching temperature. More steel elements

dissolve into matrix at higher temperatures.

Table 3. Lattice constant of the quenched steel

Quenching Temperature / °C	Fe ₍₂₀₀₎	Fe ₍₂₁₁₎	Fe ₍₂₂₀₎	Average
840	0.28741	0.28716	0.28708	0.28722
900	0.28733	0.28738	0.28734	0.28748
1050	0.28805	0.28779	0.28767	0.28783
1100	0.28804	0.28798	0.28772	0.28791
1150	0.28811	0.28783	0.28781	0.28792

Among all the elements studied, carbon contributes more to the change of lattice constant than other elements do. If the effects of other steel elements on the matrix's lattice constant are neglected, then according to Ref. [15], the relationship between the lattice constant (c) and the mass fraction (x) of carbon in the steel matrix can be given by

$$c = a_0 + 0.116x \quad (1)$$

where a_0 is the lattice constant of pure iron. The value of which is 0.28664 nm. Based on Eq. (1), the mass

fraction of carbon in the matrix of steels quenched at different temperatures can be calculated; the results are given in Table 4. It shows that the carbon mass fraction increases from the lowest value of 38% at the quenching temperature of 840°C to the highest value of 98% at the quenching temperature of 1150°C. At 840°C, 62% carbon is in a form of carbides and only 38% carbon dissolves in matrix. But when the temperature is increased to 1150°C, only 2% carbon is in the form of carbides, causing a rapid decrease in the hardness of the steel.

Table 4. Mass fraction of carbon in matrix of the steel quenched at different temperatures

Temperatures / °C	840	900	1050	1100	1150
Mass fraction of carbon / %	38	6	85	93	98

3.5. TEM results

The typical TEM micro-structures for steels quenched at different temperatures are illustrated in Fig. 5. It shows that different kinds of carbides are presented in the steel quenched at 840°C. They included spherical $M_{23}C_6$ with a size of more than 1 μm and columnar carbide clusters of hundreds nano-meters in size. These are the original carbides formed during sintering. They are still present after heat treatment because the quenching temperature

used is not high enough to turn them into other carbides or make them dissolve into the matrix. The steel quenched at 1150°C contains less carbides as compared with that quenched at 840°C. Most of the carbides are spherical in shape with a size only in the range of 10 to 200 nm. These carbides are distributed only at grain boundaries. Most of these carbides are $M_{23}C_6$. The amount of these carbides is too small to be detected by XRD diffraction.

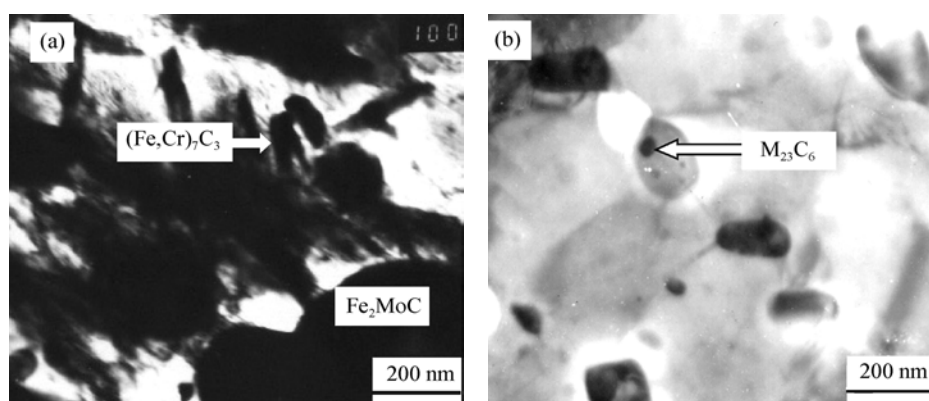


Fig. 5. TEM images of the steel quenched at different temperatures: (a) 840°C; (b) 1150°C.

3.6. Thermo-dynamics of phase transformation in quenched steel

Thermo-calc was used to study the phases that may form in the steel at different temperatures. The results of this analysis are given in Table 5. It shows that, for

steels quenched at 840°C, the carbides that can form at equilibrium are $M_{23}C_6$, κ carbide *etc.* However, $(\text{Fe,Cr})_7\text{C}_3$ and Fe_2MoC are present in addition to those predicted by the calculations. This perhaps is because the holding time used is not long enough for

the carbides to transform into the carbides calculated at equilibrium. It is expected that most of the carbides would be transformed into the equilibrium carbides at this temperature if the holding time is sufficiently long.

Table 5. Phases predicted by Thermo-calc at different temperatures

Temperature / °C	Phases
840	Ferrite, austenite, $M_{23}C_6$, κ carbide
1000	austenite, M_7C_3 , κ carbide
1100	austenite
1150	austenite

According to the calculations, the equilibrium phase of the steel at 1150°C would be austenite and no carbides are expected in the steel. This is roughly consistent with TEM observations for the steel quenched at this temperature (see Fig. 5). But TEM results show that there are small amount of $M_{23}C_6$ present at grain boundaries. $M_{23}C_6$ is a mediate phase in the process of austenite transformation. If the holding time is adequately long, all $M_{23}C_6$ would dissolve in the matrix, forming austenite. The evolution of carbides in austenite at elevated temperatures was studied by other investigations [16-19] and it was reported that the order of easiness of dissolution of carbides in austenite is $MC > M_6C (M_2C) > M_7C_3 > M_{23}C_6$, which is consistent with the observation of this study.

4. Conclusions

The hardness of the quenched steel increases with increasing quenching temperature in the range of 840-900°C, but remains almost constant in the range of 900-1100°C. When the quenching temperature is higher than 1100°C, the hardness decreases as the quenching temperature increases.

Quenching temperature greatly affects the carbon mass fraction in the matrix of the quenched steel. The carbon dissolved in the matrix is just 0.38 when quenched at 840°C. But it is 0.98 when quenched at 1150°C.

Most of the carbides formed during sintering can not dissolve into the matrix of the steel when the steel is heat treated at relatively low temperatures. At a higher heat treatment temperature, such as 1150°C, most of the carbides dissolved into the steel matrix with just a small amount of tiny spherical $M_{23}C_6$ present at grain boundaries.

Reference

[1] T. Ootani, N. Yahata, A. Fujiki, and A. Ehira, Impact wear

- char acteristics of engine valve and valve seat insert materials at high temperature, *Wear*, 188(1995), No.1-2, p.175.
- [2] T. Tetsui, Gamma Ti aluminides for non-aerospace applications, *Curr. Opin. Solid State Mater. Sci.*, 4(1999), p.243.
- [3] A. Kawana, Development of PVD ceramic coatings for valve seats, *Surf. Coat. Technol.*, 86-87(1996), p.212.
- [4] B.S. Mann, High temperature friction and wear characteristics of various coating materials for steam valve, *Wear*, 240(2000), p.223.
- [5] S. Hogmark, Tribological properties of thin hard coatings-demands and evaluation, *Surf. Coat. Technol.*, 90(1997), p.247.
- [6] X.M. Yang, Development and application of engine valve seat materials, *J. Wuhan Univ. Automob. Eng.* (in Chinese), 120(1998), No.3, p.61.
- [7] S.Q. Zhao and S.Q. Li, A study on the new material for valve seat insert and its wear resistance in IC engine, *Combust. Eng.*, 10(1989), No.1, p.57.
- [8] Y.H. Zhang, Development of high wear resistance valve/valve seat steel, *Int. Combust.*, 48(1999), p.64.
- [9] Y.T. Guo, Design of valve/valve seat steel for diesel engine, *Automob. Technol. Mater.* (in Chinese), 1997, No.6, p.30.
- [10] S.L. Zhang, X.J. Sun, and H. Dong, Effect of deformation on the evolution of spheroidization for the ultra high carbon steel, *Mater. Sci. Eng. A*, 432(2006), p.324.
- [11] H.J. Li, B.Q. Wang, X.Y. Song, S.Z. Guo, and N.J. Gu, New spheroidizing technique of ultra-high carbon steel with aluminum addition, *J. Iron Steel Res. Int.*, 13(2006), No.3, p.9.
- [12] J.W. Zhu, Y. Xu, and Y.N. Liu, Lath martensite in 1.4%C ultra-high carbon steel and its grain size effect, *Mater. Sci. Eng. A*, 385(2004), p.440.
- [13] N. Chen, H.Z. Liang, and R.X. Li, Application of computer to precise calculation of lattice constant, *Comput. Appl. Chem.*, 19(2002), No.3, p.207.
- [14] C.X. Wu and S.R. Chen, Precise measurement of lattice constant of tungsten and cobalt, *Rare Met. Cem. Carbides* (in Chinese), 1999, No.4, p.30.
- [15] L. Qiu and Y.H. Hu, *XRD Technology and Equipments* (in Chinese), Metallurgical Industry press, Beijing, 1998, p.261.
- [16] D.V. Shtansky and G. Inden, Phase transformation in Fe-Mo-C and Fe-W-C steels—II. Eutectoid reaction of $M_{23}C_6$ carbide decomposition during austenitization, *Acta Mater.*, 45(1997), p.2879.
- [17] N.C. Law and S.A. Parsons, Crystallography of carbide precipitation at transformation interfaces during austenite decomposition in a low-steel steel, *Mater. Sci. Technol.*, 3(1987), p.642.
- [18] S.K. Sahay, H.K.D.H. Bhadeshia, and R.W.K. Honeycombe, Carbide precipitation and the nucleation of allotriomorphic ferrite in an Fe-W-C steel, *Mater. Sci. Eng. A*, 157(1992), p.101.
- [19] D.V. Shtansky and G. Inden, Phase transformation in Fe-Mo-C and Fe-W-C steels—I. The structural evolution during tempering at 700°C, *Acta Mater.*, 45(1997), p.2861